Key Points:
- The vertical distribution of methane after surface emission on Mars is simulated
- Vertical layers of methane can be formed during the first weeks after the emission
- Detection of such layers will provide strong indication of recent surface release

Supporting Information:
- Supporting Information S1
- Movie S1
- Movie S2

Correspondence to:
S. Viscardy,
sebastien.viscardy@aeronomie.be

Formation of layers of methane in the atmosphere of Mars after surface release

S. Viscardy[1], F. Daerden[1], and L. Neary[1]

[1]Royal Belgian Institute for Space Aeronomy BIRA-IASB, Brussels, Belgium

Abstract Simulations with a general circulation model for the atmosphere of Mars show that surface emissions of methane can result in a highly nonuniform vertical distribution throughout the atmosphere, including the formation of layers, during the first weeks after the release. The fate of the released methane is determined by the global circulation pattern at the time of the release, and the methane can be transported to locations over the planet that are remote from the emission site. It typically takes several weeks for the methane to become more uniformly mixed, implying that the detection of vertical layers of methane can be indicative of recent surface emission. This puts the existing observations in a new perspective and will allow instruments on the upcoming ExoMars Trace Gas Orbiter mission to detect signatures of surface emission activity as they are designed to measure the first vertical profiles of methane on Mars.

1. Introduction

The presence of methane (CH_4) on Mars has gained strong interest through repeated reports of its detection since 2003 [*Formisano et al.*, 2004; *Krasnopolsky et al.*, 2004; *Mumma et al.*, 2009; *Fonti and Marzo*, 2010; *Geminale et al.*, 2011; *Krasnopolsky*, 2012; *Webster et al.*, 2015] and the possible implications for geophysical or biological activity on Mars. As methane is a reduced gas it is photochemically not stable in the highly oxidizing Martian atmosphere, its lifetime is of the order of a few hundred years, assuming that the methane is destroyed only by the known photochemical processes [*Summers et al.*, 2002]. As a result, any presence of methane would point to more recent activity. Several processes that can create methane on Mars have been proposed over the past decade. One of the most likely sources for the atmospheric methane was that it was released from subsurface reservoirs by release through pores in the surface [*Mumma et al.*, 2009]. While *Zahnle et al.* [2011] disputed the presence of methane on Mars, both by challenging the correctness of the retrieval process of *Mumma et al.* [2009], an argument rebutted by *Villanueva et al.* [2013], and by putting forward theoretical arguments, they in fact did not rule out rare emission events. A problematic issue raised by the observations of 2006 reported in *Mumma et al.* [2009] was that these represented a reduction of the atmospheric methane content by a factor of 3 in 3 years time, inconsistent with the long photochemical lifetime. This was confirmed by numerical simulations with a general circulation model (GCM) for Mars [*Lefèvre and Forget*, 2009]. Since then a range of strong destruction mechanisms for methane has been proposed [e.g., *Knak Jensen et al.*, 2014; *Holmes et al.*, 2015], but the issue is not solved today, also due to lack of new observations during a long time period. *Villanueva et al.* [2013] did not report any methane above ~7 parts per billion (ppb) in the time period 2006–2010, while *Geminale et al.* [2011] reported higher values in this time period measured by the Planetary Fourier Spectrometer (PFS) on Mars Express, but only in regions with very low signal-to-noise ratio, increasing their uncertainty. *Krasnopolsky* [2012] reported a very localized measurement of 10 ppb in 2006, but no values exceeding 8 ppb since then.

The in situ measurements by the Tunable Laser Spectrometer (TLS) of the Sample Analysis at Mars (SAM) on Curiosity represented a strong affirmation of the presence of methane on Mars in 2013–2014 [*Webster et al.*, 2015] and showed a nonuniform trend of methane throughout the year, supporting the idea of intermittent methane release. It was, however, not immediately clear how representative these near-surface measurements inside a crater are for the atmospheric peak and background methane content. *Moore et al.* [2016] found evidence of reduced mixing between air inside and above Gale crater by comparing dust measurements from different instruments on Curiosity. Until present nothing is known about the vertical distribution of methane at the times of any of the positive detections. GCM studies of surface release of methane focused on its horizontal spreading [*Lefèvre and Forget*, 2009; *Mischna et al.*, 2011; *Holmes et al.*, 2015].

The upcoming European Space Agency (ESA)/Roskosmos ExoMars Trace Gas Orbiter (TGO) mission (launch foreseen in March 2016) carries two instruments that are designed to measure the first vertical profiles of methane with high sensitivity and to do so in a mode of systematic diurnal monitoring throughout a full Mars year. These are the Nadir and Occultation for Mars Discovery (NOMAD) spectrometer suite [*Vandaele et al.*, 2015], with expected detection limit for methane of 25 parts per trillion by volume and a vertical resolution of ~1 km, and the Atmospheric Chemistry Suite (ACS) [*Korablev et al.*, 2015]. In anticipation of their measurements it is important to better understand the behavior of methane also in the vertical after an emission from the surface. This is the purpose of the present report in which we present some simple methane release experiments in a GCM and analyze the resulting vertical distribution of methane.

2. Global Circulation Model

The general circulation model for the atmosphere of Mars applied here is described in *Daerden et al.* [2015]. It is a grid point model based on the Canadian Global Environmental Multiscale model for weather forecasting on Earth [*Côté et al.*, 1998; *Moudden and McConnell*, 2005]. For the present study it was operated at $4° \times 4°$ horizontal resolution and with 102 vertical levels reaching from the surface to 8×10^{-6} Pa (~150 km). Geophysical boundary conditions were applied for topography [*Smith et al.*, 1999], albedo [*Christensen et al.*, 2001], thermal inertia [*Putzig et al.*, 2005], and roughness length [*Hébrard et al.*, 2012]. The model simulated an annual CO_2 ice mass cycle that is in agreement with the observations by the Gamma Ray Spectrometer on the NASA Mars Odyssey mission [*Kelly et al.*, 2006] and interactively it simulated a surface pressure cycle in agreement with the measurements on the NASA Viking Lander 1 mission [*Hess et al.*, 1976]. Size-distributed dust was lifted by saltation and dust devils and was radiatively active [*Daerden et al.*, 2015]. The simulated annual global dust cycle compared well to the trend of the observations by the Thermal Emission Spectrometer (TES) [*Smith*, 2004] on board Mars Global Surveyor.

Methane is a buoyant gas, with a molecular mass (16 atomic mass units, amu) that is lower than that of the CO_2-rich air (44 amu). This will have an important effect on the air immediately after the methane emission; however, we will assume that on the coarse scale of the model grid, this effect is not resolved and methane will be well mixed with air inside a model grid cell after being emitted. Methane is then subject to convective mixing in the planetary boundary layer (PBL) and will mix up rapidly to the top of the PBL that can reach up to ~10 km at low latitudes on Mars. Methane will be taken up by the general circulation and will be further advected using the resolved model wind fields. Molecular diffusion acts on the different gases inside a grid cell in the model following the expression of *Davis* [1982], but this only has a nonnegligible effect at heights above ~100 km [e.g., *Rodrigo et al.*, 1990].

The most important fields that govern the evolution of methane throughout the atmosphere after emission are the wind fields. As there are no global direct wind observations available for Mars, the simulations were evaluated with the Mars Analysis Correction Data Assimilation (MACDA) data set [*Montabone et al.*, 2014]. MACDA is a reanalysis of observations of total dust optical depth and of vertically resolved atmospheric temperatures from TES. Atmospheric winds are mainly controlled by the atmospheric temperatures, and the accuracy of atmospheric temperatures is highly improved by the assimilation of TES data [*Lewis et al.*, 2007]. Both zonal and meridional winds in MACDA and in the simulations have been averaged zonally and over a $10°$ L_s period starting at the time of the emission. The comparison presented in the supporting information (Figure S1) is satisfactory both for the strength of the winds and for their distribution across latitude and height, and sufficient for the purposes of this paper.

3. Simulations

Because of the sparsity of the available methane observations, the paper focuses on the qualitative evolution of the methane and avoids an exhaustive presentation of many possible emission scenarios. In the main simulation the emission was done at Nili Fossae (78°E, 22°N) at solar longitude $L_s = 150°$, a choice inspired by the observations of *Mumma et al.* [2009]. This emission was found to be illustrative of emissions at other times and places and captured some of the most interesting behavior of methane after surface release. Initially, the surface emission was assumed to be instantaneous, i.e., all methane was emitted during one model time step of 30 Mars minutes (1/48 of a Mars solar day or sol), and the time of emission was local noon. The area over which the methane was released spanned one single grid cell measuring $4° \times 4°$ in latitude and
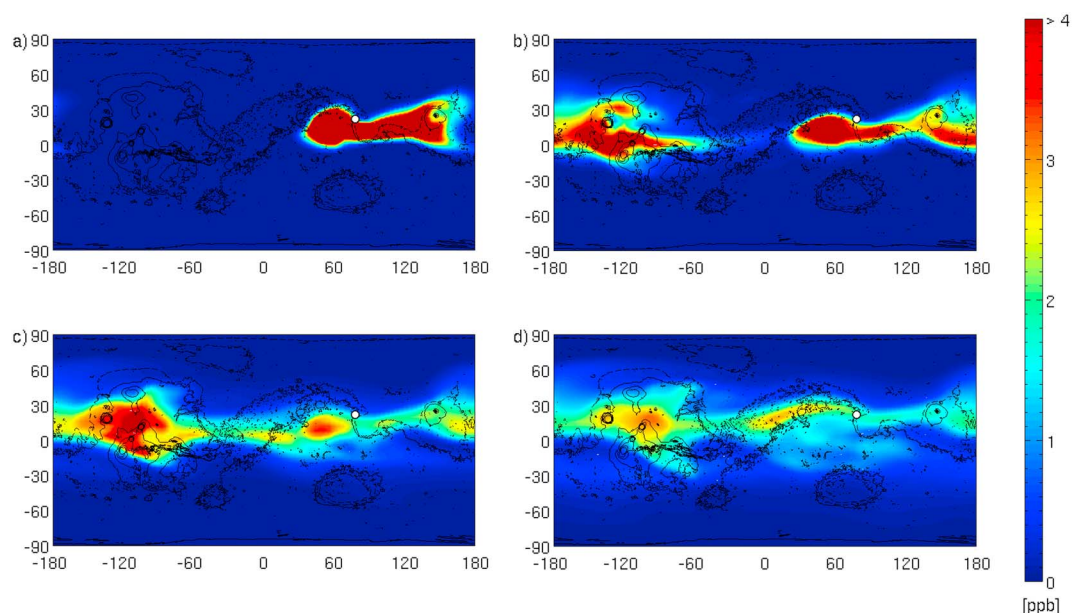
Figure 1. Horizontal distribution of the column-averaged mixing ratio of methane (in ppb) for (a) 5, (b) 10, (c) 15, and (d) 20 sols after an instantaneous surface release of methane in Nili Fossae (indicated by a white dot) at $L_s = 150°$.

longitude (~220 km × 237 km at the emission site). The methane was released in the lowest model grid level that reached up to 38.9 m above the surface at the time of emission, and it was assumed that the released gas was at the same temperature and pressure as the air in this lowest model level in order to avoid complications due to buoyancy effects. The amount of released gas was set at 5×10^6 kg, i.e., ~10% of the total atmospheric mass of methane estimated by *Mumma et al.* [2009] in 2003. The actual amount of emitted gas is not critical for the present study which only focuses on the qualitative aspects of the dispersion of the gas throughout the atmosphere. Initially, it was also assumed that there is no methane present in the atmosphere at the time of the release. We investigated the evolution of the released methane over the course of 20 sols. For that reason, photochemistry or other loss processes were not taken into account.

The simulated horizontal evolution of the column-averaged mixing ratio of methane (the ratio of the vertically integrated number densities of methane and carbon dioxide) is plotted in Figure 1 in steps of 5 sols after emission. During the very first sols, the methane cloud moved mainly in a southwest direction up to a region centered around 60°E, 15°N (between Terra Sabaea and Syrtis Major) where it resided for several sols before a second component of the methane cloud developed east of the emission location which was easily seen 5 sols after the release (Figure 1a). Ten sols after release, the bulk part of the cloud had gradually become more diffuse, while the eastern component continued to develop eastward just north of the equator (Figure 1b). In the following 5 sols this evolution continued, and the methane cloud had completed one turn around the planet along the equator (Figure 1c). Twenty sols after emission, no indication of the location of the emission site remained (Figure 1d). The meridional dispersion of the methane to higher latitudes was much slower than the zonal transport. The local maxima in the methane column-averaged mixing ratio at low northern latitudes are similar to those achieved in the simulations of *Holmes et al.* [2015] that were found to match with the observational data of *Fonti and Marzo* [2010] and were caused by a topography-induced stationary wave [*Holmes et al.*, 2015].

Figure 2 shows the simulated vertical evolution of the methane. To capture the three-dimensional evolution of the methane, we provide plots of both zonally averaged volume mixing ratios (vmr) of methane (averaged over all longitudes; Figures 2a, 2c, 2e, and 2g) and meridionally averaged methane vmr (averaged over all latitudes, Figures 2b, 2d, 2f, and 2h). The zonal mean plots also show contour lines of the zonally averaged mass stream function as computed from the simulations, averaged over the 5 sols precedent to the time of the plot. This quantity is useful to understand the evolution of methane once it had ascended above the PBL. When considering the net circulation over several days and nights, two main circulation cells of equal size appeared, one on either side of the equator (Figures 2a, 2c, 2e, and 2g). Their resulting effect was to lift the
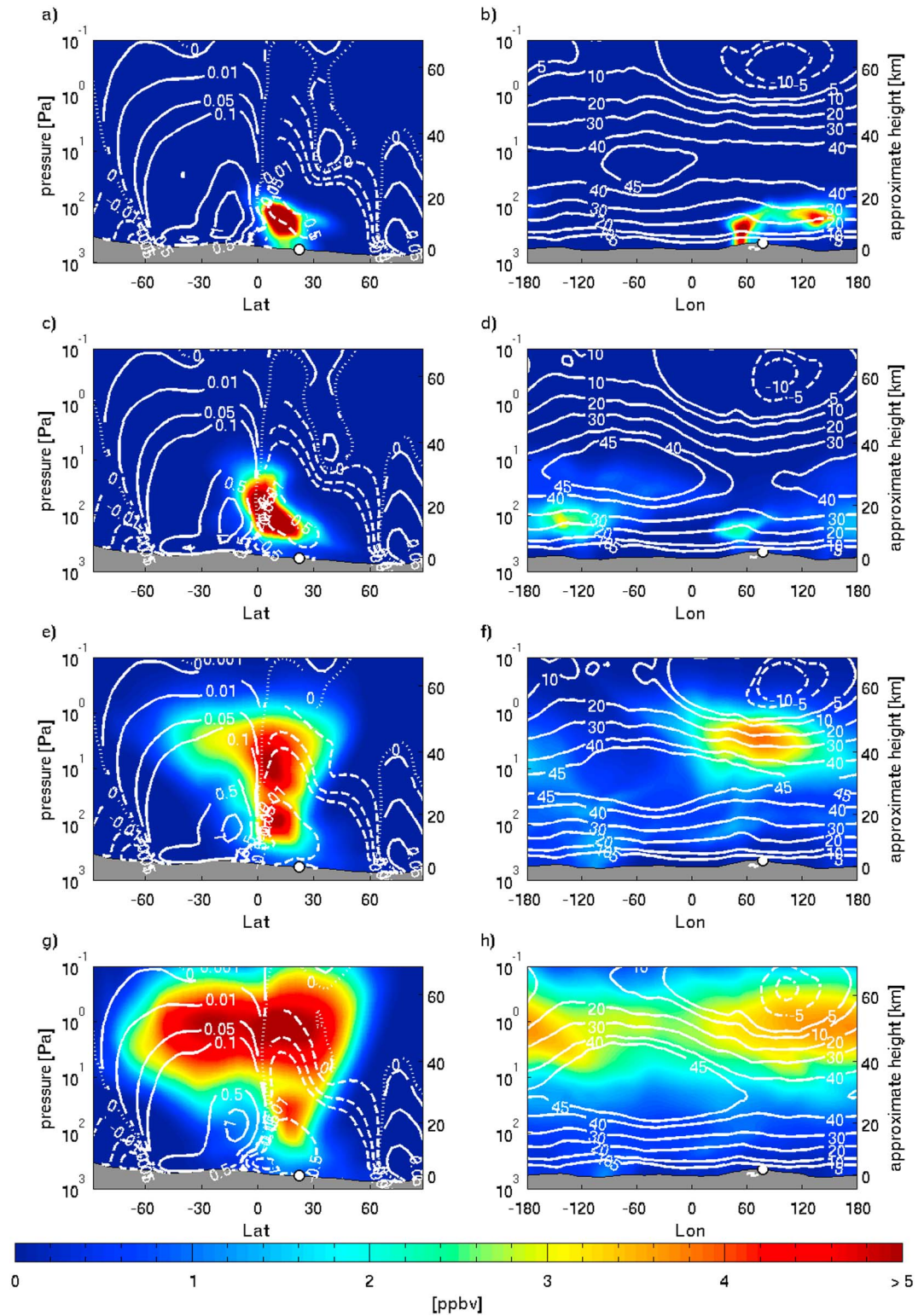
Figure 2. Vertical distribution of methane volume mixing ratio (vmr) in ppbv for (a, b) 5, (c, d) 10, (e, f) 15, and (g, h) 20 sols after the surface emission at Nili Fossae (indicated with a white dot). Figures 2a, 2c, 2e, and 2g show zonal mean methane vmr with contour lines of the mass stream function ($\times 10^9$ kg/s) zonally averaged over the planet and over the five preceding sols. Full lines represent counterclockwise movement, and dashed lines represent clockwise movement of air. Figures 2b, 2d, 2f, and 2h show meridional mean methane vmr with contour lines added of the zonal component of the wind fields averaged over all latitudes and over the five preceding sols. Westerlies and easterlies are, respectively, represented by the full and dashed lines.
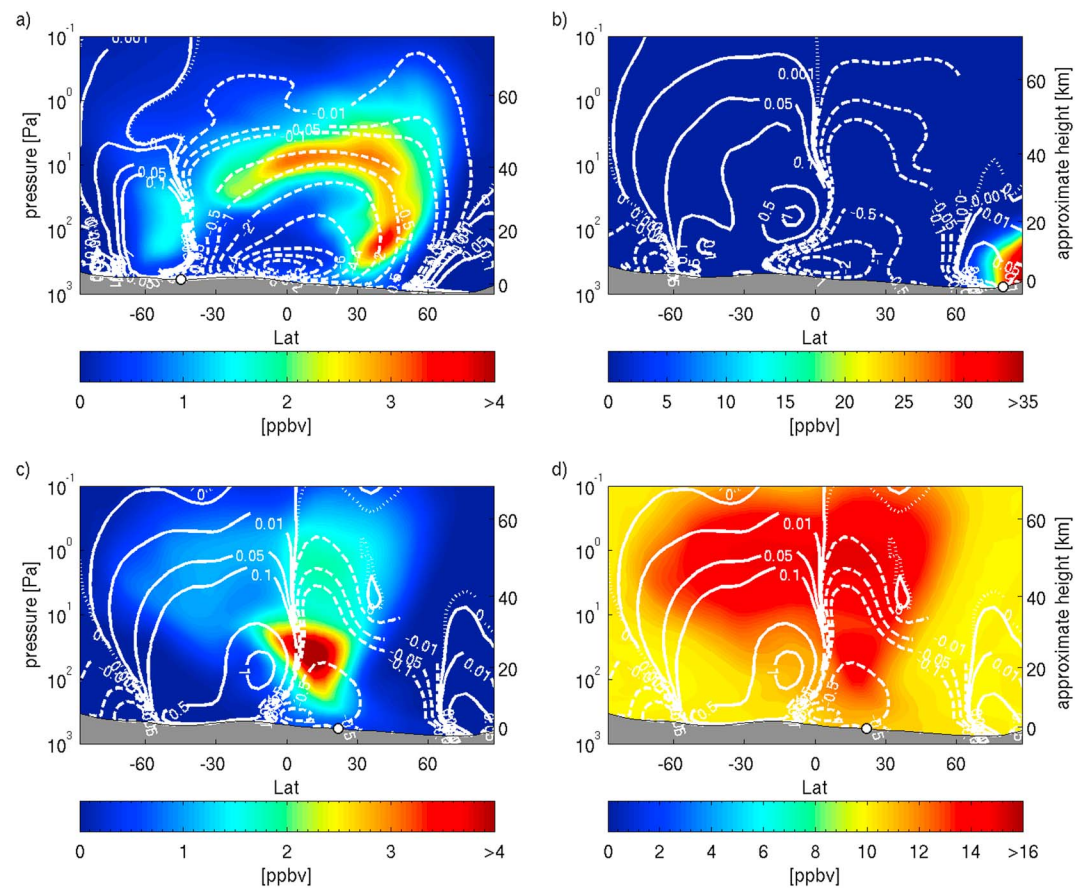
Figure 3. Zonal mean vmr of methane 20 sols after surface release for several simulations. (a) Instantaneous release from 240°E, 45°S at $L_s = 220°$. (b) Instantaneous release from 240°E, 80°N at $L_s = 170°$. (c) Continuous release over 10 sols from 78°E, 22°N starting at $L_s = 150°$. The plot is for 20 sols after the start of the release. (d) Instantaneous surface emission of methane from 78°E, 22°N at $L_s = 150°$, in a preexistent uniform background abundance of 10 ppbv. The emission site is indicated by a white dot in all plots. Contour lines of the mass stream function ($\times 10^9$ kg/s) are added as in Figure 2.

air from the lower atmosphere at low latitudes and to transport it upward and to higher latitudes. The meridional mean plots have contour lines of the simulated zonal winds, averaged over the same time period, indicating the wind strength variation with height. These highlight the presence of strong zonal jets at 30–40 km height.

In addition to Figure 2, an animation of the simulated zonal mean methane vmr with a high time resolution is available in the supporting information (Movie S1). After release at local noon, the methane was rapidly mixed in the vertical due to the turbulent convection in the PBL and reached the top of the PBL (~11 km) around 3 P. M.. When the PBL turbulence decreased in the late afternoon, the methane distribution remained steady with a slow descent at night as the atmosphere cooled down. As reported above, the released methane drifted to the southwest during the first few sols. By 5 sols after emission, part of the methane had risen to above the top of the PBL due to the upwelling branch of the Hadley circulation (Figure 2a). Due to the differential advection and the westerly winds, the methane was drawn out in a layer at ~15 km height in a direction east of the emission location (Figure 2b), explaining the eastern outflow reported above. Over the next 5 sols the methane continued to ascend above the equator following the streamlines (Figure 2c) while it continued to move eastward (Figure 2d). Fifteen sols after the release, the methane had reached heights up to 40 km where the zonal jets were of maximal strength and the dispersion process accelerated. The vertical distribution of the methane vmr was still highly nonuniform and showed distinct detached vertical layers (Figures 2e and 2f). At the end of the first 20 sols, the methane started to become more dispersed toward higher latitudes following the streamlines (Figure 2g) and had completed over one circle around the planet (Figure 2h). As the atmospheric circulation dispersed the methane further over the next weeks, the distribution of methane became gradually more uniform over the entire atmosphere.

The mechanism described above is general and occurs in many cases. Results from a second simulation are shown in Figure 3a, in which the same amount of methane (5×10^6 kg) was released from 240°E, 45°S at $L_s = 220°$, a region and time of year where methane was reported to have been detected in 2005 [*Mumma et al.*, 2009]. (More results of this simulation are shown in Figures S2 and S3 and in Movie S2 in the supporting information.) At this season (southern spring) two main circulation cells controlled the meridional transport: a small cell in the Southern Hemisphere and another much larger cell which transported the air from the Southern to the Northern Hemisphere. After methane was released from the surface at latitude 45°S, the southern cell moved the methane slightly to the north until it reached ~40°S, which corresponded to the latitude of the intersection between the two major circulation cells. This step took ~5 sols (Figures S3a and S3b). Then methane was gradually lifted upward and moved northward following the largest circulation cell (Figures S3c and S3d). This process continued over the following sols (Figures S3e and S3f). Twenty sols after release, distinct layers of methane were present in the atmosphere, roughly following the streamlines of the circulation cells (Figures 3a, S3g, and S3h), up to heights of 40 km. Most strikingly, the methane had moved to the Northern Hemisphere, remote from the emission location at 45°S.

4. Discussion

In general, the fate of methane after release will be governed by the actual global circulation pattern at the place and time of the emission. It will follow the upwelling branches of the Hadley circulation cells, and its spread along longitudes will speed up if it encounters strong zonal jets at typically 40 km height. For an atmospheric mass flux of 0.5×10^9 kg/s at the upwelling branch of the Hadley cell to transport 5×10^6 kg of methane, it takes ~6 sols, assuming the methane vmr is 50 parts per billion by volume (ppbv). At 40 km, for a typical meridional wind strength of 3 m/s (Figure S1), methane can be transported from the equator to 45°N in ~10 sols, and for a zonal wind strength of 50 m/s (Figure 3f), it takes ~5 sols for methane to complete one circle around the planet. These numbers provide the time scales at which the layers of methane are typically formed, and they will also disperse on such time scales, i.e., they are transient in nature on the time scale of a few weeks at most. As such, these layers of methane are signatures of surface emission that occurred on the scale of days or weeks prior to their formation.

There are also examples of emissions which do not lead to dispersion throughout the atmosphere and the formation of layers. For example, the circulation in the polar region during local summer is such that any methane that is released there will remain in the polar region. A third simulation was performed where 5×10^6 kg of methane was released from the surface at 240°E, 80°N at $L_s = 170°$ (late summer), a time and place suggested as a possible source of methane from analysis of measurements by PFS [*Geminale et al.*, 2011; M. Giuranna, personal communication]. Figure 3b shows the distribution of methane after 20 sols, barely any methane had left the polar region and remained constrained to below 20 km.

In the previous simulations an instantaneous release of the total amount of methane was assumed, but the release could also be slow over a longer time period. The simulations were repeated but with methane continuously released with a constant flux over a period of 10 sols, in the end accumulating to the same total amount of 5×10^6 kg. Figure 3c shows the vertical distribution of methane 20 sols after the start of such a continuous release from Nili Fossae at $L_s = 150°$. When comparing with the case of an instantaneous release (Figure 2g), the layers were less distinct at this time. The methane was dispersed similarly as the atmospheric circulation was identical, and the shape of the methane cloud is similar to that of the case of instantaneous release, but as the release lasted for a longer time with a lower flux, more methane is located at lower heights.

All these simulations were also repeated with a background of 10 ppbv of methane uniformly present in the atmosphere at the time of the emission. The resulting vertical distribution of methane for the instantaneous release from Nili Fossae is shown in Figure 3d. The same patterns as for the simulation with zero background are reproduced (Figure 2g), and the resulting distribution of methane was merely the sum of the preexisting background and the released methane, i.e., the presence of a uniform background of methane does not impact on the conclusions of our study.

The NOMAD and ACS instruments on TGO are designed to provide the first vertical profile measurements of methane on Mars by applying the highly sensitive solar occultation technique [*Vandaele et al.*, 2015; *Korablev et al.*, 2015]. NOMAD is planned to measure two vertical profiles per orbit at latitudes that vary smoothly

throughout the Martian year [*Vandaele et al.*, 2015]. With 12 orbits per day, for a specific day of the year, NOMAD will sample 12 profiles located at one latitude and another 12 profiles at a different latitude, with a spacing of ~30° in longitude between them at each of the two latitudes. As our simulations show that methane released from the surface disperses rapidly over the planet, a daily sampling of 12 longitudes at two latitude bands will lead to a high likelihood of detecting a signature of any surface emission and will even allow the evolution of the released methane to be followed. GCM simulations can then be used to trace the methane back in time to confine the time of the release, if not the location of the source. Tracing methane emissions on Mars and locating their sources was originally foreseen to be the objective of the nadir IR channel of NOMAD [*European Space Agency* (ESA), 2010; *Zurek et al.*, 2011; *Vandaele et al.*, 2015]. However, the descope of a cryoradiator due to mass constraints reduced the sensitivity of this nadir channel [*Vandaele et al.*, 2015]. The present work shows how the solar occultation channel can complement the nadir channel for the monitoring of methane surface emissions. As the TGO instruments will not only measure methane but also temperature, dust, ice clouds, and various chemical constituents including water vapor, the measurements can also help to investigate whether such methane layers originate from the dynamical process described in this report or that they may possibly have another physical or chemical explanation, such as the evaporation of airborne methane clathrates [*Chassefière*, 2009].

5. Conclusions

A general circulation model for the atmosphere of Mars has been applied to simulate surface emission of methane and to investigate its vertical distribution during the first weeks after the release. Such surface emissions had been suggested to explain observations of methane. Previous GCM simulations have focused on the horizontal evolution of the methane, but the present study focuses on the three-dimensional dispersion of methane throughout the atmosphere after the surface release. It is found that a highly nonuniform vertical distribution, including distinct vertical layers, can appear throughout the atmosphere during the first weeks after the emission. This is explained by the global circulation patterns in the atmosphere at the time of the emission. Large Hadley cells transport the methane rapidly to other locations over the planet, and methane will be stretched out in layers along the general circulation streamlines at heights corresponding to strong zonal jets.

This result puts previous observations in a different perspective. All observations to date except the ones by TLS-SAM measured the total column abundance of methane, but the derivation of the local mixing ratio is not well constrained. If the methane vertical profile has a distinct maximum away from the surface, the vmr at this maximum will be considerably higher than the column-averaged mixing ratio. For the measurements by TLS-SAM our finding indicates that abundances of methane higher up in the atmosphere can be much larger than those measured at the surface.

Our simulations show that measurements of nonuniform vertical distributions and distinct vertical layers of methane can have a purely dynamical explanation and can be indicative of very recent surface emission. The ExoMars TGO mission carries two instruments that can measure the vertical profile of methane on Mars and will monitor this on a daily basis at the global scale. As such, this finding contributes to addressing one of the main scientific objectives of the ExoMars TGO mission, i.e., the search for signs of active release of methane on Mars [*ESA*, 2010; *Zurek et al.*, 2011].

References

Chassefière, E. (2009), Metastable methane clathrate particles as a source of methane to the Martian atmosphere, *Icarus*, *204*, 137–144, doi:10.1016/j.icarus.2009.06.016.

Christensen, P. R., J. L. Bandfield, V. E. Hamilton, and S. W. Ruff (2001), Martian water cycle modeling with the second generation of the global Mars multiscale model, *J. Geophys. Res.*, *106*, 23,823–23,872, doi:10.1029/2000JE001370.

Côté, J., S. Gravel, A. Méthot, A. Patoine, M. Roch, and A. Staniforth (1998), The operational CMC MRB Global Environmental Multiscale (GEM) model. Part I: Design considerations and formulation, *Mon. Weather Rev.*, *126*, 1373, doi:10.1175/1520-0493(1998)126<1373:TOCMGE>2.0.CO;2.

Daerden, F., J. A. Whiteway, L. Neary, L. Komguem, M. T. Lemmon, N. G. Heavens, B. A. Cantor, E. Hébrard, and M. D. Smith (2015), A solar escalator on mars: Self-lifting of dust layers by radiative heating, *Geophys. Res. Lett.*, *42*, 7319–7329, doi:10.1002/2015GL064892.

Davis, E. J. (1982), Transport phenomena with single aerosol particles, *Aerosol Sci. Technol.*, *2*, 121–144, doi:10.1080/02786828308958618.

European Space Agency (ESA) (2010), ExoMars Trace Gas Orbiter announcement of opportunity. [Available at http://exploration.esa.int/mars/46297-ao-for-exomars-orbiter-instruments/.]

Fonti, S., and G. A. Marzo (2010), Mapping the methane on Mars, *Astron. Astrophys.*, *512*, A51, doi:10.1051/0004-6361/200913178.

Formisano, V., S. Atreya, T. Encrenaz, N. Ignatiev, and M. Giuranna (2004), Detection of methane in the atmosphere of Mars, *Science*, *306*, 1758–1761, doi:10.1126/science.1101732.

Geminale, A., V. Formisano, and G. Sindoni (2011), Mapping methane in Martian atmosphere with PFS-MEX data, *Planet. Space Sci.*, *59*, 137–148, doi:10.1016/j.pss.2010.07.011.

Hébrard, E., C. Listowski, P. Coll, B. Marticorena, G. Bergametti, A. Määttänen, F. Montmessin, and F. Forget (2012), An aerodynamic roughness length map derived from extended Martian rock abundance data, *J. Geophys. Res.*, *117*, E04008, doi:10.1029/2011JE003942.

Hess, S. L., et al. (1976), Preliminary meteorological results on Mars from the Viking 1 lander, *Science*, *193*, 788–791.

Holmes, J. A., S. R. Lewis, and M. R. Patel (2015), Analysing the consistency of Martian methane observations by investigation of global methane transport, *Icarus*, *257*, 23–32, doi:10.1016/j.icarus.2015.04.027.

Kelly, N. J., W. V. Boynton, K. Kerry, D. Hamara, D. Janes, R. C. Reedy, K. J. Kim, and R. M. Haberle (2006), Seasonal polar carbon dioxide frost on Mars: CO_2 mass and columnar thickness distribution, *J. Geophys. Res.*, *111*, E03S07, doi:10.1029/2006JE002678.

Knak Jensen, S. J., et al. (2014), A sink for methane on Mars? The answer is blowing in the wind, *Icarus*, *236*, 24–27, doi:10.1016/j.icarus.2014.03.036.

Korablev, O. I., F. Montmessin, A. A. Fedorova, N. I. Ignatiev, A. V. Shakun, A. V. Trokhimovskiy, A. V. Grigoriev, K. A. Anufreichik, and T. O. Kozlova (2015), ACS experiment for atmospheric studies on "ExoMars 2016" orbiter, *Solar Syst. Res.*, *49*(7), 529–537, doi:10.1134/S003809461507014X.

Krasnopolsky, V. A. (2012), Search for methane and upper limits to ethane and SO_2 on Mars, *Icarus*, *217*, 144–152, doi:10.1016/j.icarus.2011.10.019.

Krasnopolsky, V. A., J. P. Maillard, and T. C. Owen (2004), Detection of methane in the Martian atmosphere: Evidence for life? *Icarus*, *172*, 537–547, doi:10.1016/j.icarus.2004.07.004.

Lefèvre, F., and F. Forget (2009), Observed variations of methane on Mars unexplained by known atmospheric chemistry and physics, *Nature*, *460*, 720–723, doi:10.1038/nature08228.

Lewis, S. R., P. L. Read, B. J. Conrath, J. C. Pearl, and M. D. Smith (2007), Assimilation of Thermal Emission Spectrometer atmospheric data during the Mars Global Surveyor aerobraking period, *Icarus*, *192*, 327–347.

Mischna, M. A., M. Allen, M. I. Richardson, C. E. Newman, and A. D. Toigo (2011), Atmospheric modeling of Mars methane surface releases, *Planet. Space Sci.*, *59*, 227–237, doi:10.1016/j.pss.2010.07.005.

Montabone, L., K. Marsh, S. R. Lewis, P. L. Read, M. D. Smith, J. A. Holmes, A. Spiga, D. Lowe, and A. Pamment (2014), The Mars Analysis Correction Data Assimilation (MACDA) dataset V1.0, *Geosci. Data J.*, *1*, 129–139, doi:10.1002/gdj3.13.

Moore, C. A., et al. (2016), A full Martian year of line-of-sight extinction within Gale Crater, Mars as acquired by the MSL Navcam through sol 900, *Icarus*, *264*, 102–108, doi:10.1016/j.icarus.2015.09.001.

Moudden, Y., and J. C. McConnell (2005), A new model for multiscale modeling of the Martian atmosphere, GM3, *J. Geophys. Res.*, *110*, E04001, doi:10.1029/2004JE002354.

Mumma, M. J., G. L. Villanueva, R. E. Novak, T. Hewagama, B. P. Bonev, M. A. DiSanti, A. M. Mandell, and M. D. Smith (2009), Strong release of methane on Mars in northern summer 2003, *Science*, *323*, 1041–1045, doi:10.1126/science.1165243.

Putzig, N. E., M. T. Mellon, K. A. Kretke, and R. E. Arvidson (2005), Global thermal inertia and surface properties of Mars from the MGS mapping mission, *Icarus*, *173*, 325–341, doi:10.1016/j.icarus.2004.08.017.

Rodrigo, R., E. García-Álvarez, M. J. López-González, and J. J. López-Moreno (1990), A nonsteady one-dimensional theoretical model of Mars' neutral atmospheric composition between 30 and 200 km, *J. Geophys. Rev.*, *95*(B9), 14,795–14,810, doi:10.1029/JB095iB09p14795.

Smith, D. E., et al. (1999), The global topography of Mars and implications for surface evolution, *Science*, *284*, 1495, doi:10.1126/science.284.5419.1495.

Smith, M. D. (2004), Interannual variability in TES atmospheric observations of Mars during 1999–2003, *Icarus*, *167*, 148–165, doi:10.1016/j.icarus.2003.09.010.

Summers, M. E., B. J. Lieb, E. Chapman, and Y. L. Yung (2002), Atmospheric biomarkers of subsurface life on Mars, *Geophys. Res. Lett.*, *29*(24), 2171, doi:10.1029/2002GL015377.

Vandaele, A. C., et al. (2015), Science objectives and performances of NOMAD, a spectrometer suite for the ExoMars TGO mission, *Planet. Space Sci.*, *119*, 233–249, doi:10.1016/j.pss.2015.10.003.

Villanueva, G. L., M. J. Mumma, R. E. Novak, Y. L. Radeva, H. U. Käufl, A. Smette, A. Tokunaga, A. Khayat, T. Encrenaz, and P. Hartogh (2013), A sensitive search for organics (CH_4, CH_3OH, H_2CO, C_2H_6, C_2H_2, C_2H_4), hydroperoxyl (HO_2), nitrogen compounds (N_2O, NH_3, HCN) and chlorine species (HCl, CH_3Cl) on Mars using ground-based high-resolution infrared spectroscopy, *Icarus*, *223*, 11–27, doi:10.1016/j.icarus.2012.11.013.

Webster, C. R., et al. (2015), Mars methane detection and variability at Gale crater, *Science*, *347*, 415–417, doi:10.1126/science.1261713.

Zahnle, K., R. S. Freedman, and D. C. Catling (2011), Is there methane on Mars? *Icarus*, *212*, 493–503, doi:10.1016/j.icarus.2010.11.027.

Zurek, R. W., A. Chicarro, M. A. Allen, J.-L. Bertaux, R. T. Clancy, F. Daerden, V. Formisano, J. B. Garvin, G. Neukum, and M. D. Smith (2011), Assessment of a 2016 mission concept: The search for trace gases in the atmosphere of Mars, *Planet. Space Sci.*, *59*, 284–291, doi:10.1016/j.pss.2010.07.007.